Agricultural Robot Visual De-hazing Method Based on Image Segmentation Map

Jiang Dejing[1] Wang Shuchen[1] Zeng Yong[1,2] Sun Tao[1,3] Qing Lufang[1]

(1. *School of Mechanical and Electrical Engineering*, *Xuzhou Institute of Technology*, *Xuzhou* 221111, *China*
2. *School of Mechanical and Electrical Engineering*, *Yancheng Institute of Technology*, *Yancheng* 224003, *China*
3. *College of Mechanical and Electrical Engineering*, *Nanjing University of Aeronautics & Astronautics*, *Nanjing* 210016, *China*)

Abstract: Because of the extensive flexibility and accuracy, visual navigation technology has been widely used in the field of agriculture intelligent navigation, and many effective machine vision navigation application cases were developed. But under the condition of heavy fog, visual navigation precision is greatly decreased and the processing time in the front image is largely increased, which due to unable to obtain clear front image recently. If the front image interference by the fog is bigger, and image enhancement and recovery effect is not obvious, then it will cause navigation function failure, which results in unable to effectively positioning and navigation. And even it cannot work in serious. In order to solve this problem, this paper proposed an agricultural robot visual de-hazing method based on image segmentation map. First of all, this paper adopted the front end image blurring vision and regional segmentation, and got the atmospheric scattering function prediction value based on the segmentation map through the image brightness information. Second, the method optimized the atmospheric scattering function estimation value based on the orientation filter, which enhanced the image edge information, and further improved the fog residual problem caused by the large sky background. Finally, the front-end image de-hazing experiment was conducted based on the actual agriculture intelligent navigation platform, and the results were compared with traditional de-hazing method. The results showed that the method had high precision and real-time performance. The image de-hazing integrated indicators were improved by 28.9% and 29.1% respectively of two part of the video, and the time consumption was improved by 34.4% and 53.9% respectively.

Key words: agricultural robot; visual navigation; image de-hazing; segmentation map; orientation filter

0 Introduction

With the rapid development of modern agriculture intelligent cultivation technology, agricultural robots are widely used in crop harvest[1], farming and fertilizer[2] and fruits picking[3] as well as other occasions, drastically rising the safety and efficiency of modern agriculture[4]. Among them, the intelligent agricultural robots based on machine view navigation technology, because of easy operation and flexible usage, have obtained rapid development and application[5]. However, when operating under complex weather conditions such as rain, snow and fog, due to the degeneration of collecting images, blurry contents, lower contrast ratio and other reasons, leading to the accuracy reduction of path recognition, severe cases can cause the disorder of control system, cannot effectively work. Therefore, how to improve and enhance the effectiveness of visual images under the weather conditions (such as rain, snow and fog) is the challenge and development bottleneck faced by visual navigation robots at present.

In recent years, the researchers introduce the technology through image de-hazing technology into visual navigation system[6], effectively improving the operational accuracy of robot in rain, snow, and fog weather. According to the implementation means of image de-hazing, the current study methods can be

Received date: 2016-06-02 Accepted date: 2016-09-05
Supported by National Natural Science Foundation of China (Grant No. 51405418), Jiangsu Provincial Science and Technology Plan Project of China (Grant No. BC20140071) and Xuzhou Science and Technology Plan Project of China (Grant No. KC14GM047)
Corresponding author: Sun Tao, Associate Professor. E-mail: suntao@xzit.edu.cn. Tel: +86-137-76787095.

roughly divided into two classes[7]: one is the method based on the traditional image enhancement, such as Retinex algorithm[8]. The advantages of this kind of method are it can make use of the existing image enhancement processing method to highlight the target features and information in images. But the method neglects the causes of image degradation and loses some useful information in the process of enhancing so that the image is distorted. Another is the method based on the physical model. This kind of method analyzes the degradation mechanism in depth, builds atmospheric scattering function model, and recover the image before degradation through the function inversion. Because this kind of method considers the mechanism which fog causes image degradation, the effect of image de-hazing is good, the conservation of image information is intact[9]. Such as dark channel prior method proposed by HE et al.[10], because of this method using the statistical information of images, implementing method is simple, de-hazing effect is good, has become the research focus for the method through image de-hazing at present. But the soft matting process of this method increases the operation loss of algorithm, cannot adapt to the instantaneity demand from visual navigation system. On this basis, the literature [11] puts forward to use the orientation filter to replace the soft matting approach, but under the condition of large area of the sky background, de-hazing effect is poorer. Literature [12] by using median filter to pre-estimate the atmospheric dissipation function, effectively improving the defect of soft matting, but the fuzzy problem of filter orientation limits the improvement effect. Literature [13] mixes the two kinds of methods together, achieving the dark channel prior combined with Retinex, further rising the effect of de-hazing. Although the present research method improves the effect of image de-hazing and provides the effective thinking, but loses partial detailed information of the images after de-hazing, especially at a large area of the sky background and the combined part of the fog and target image, easily causes the larger noise interference and reduces the signal to noise ratio (SNR) of the image. It is extremely adverse for the agricultural robot navigation system which operating under a complex environment.

In order to solve this problem, this paper puts forward a kind of method ofde-hazing for agricultural robot visual based on image segmentation mapping. The close shot and distant view are segmented based on the size of images containing fog, the atmospheric dissipation function is preliminary estimated through the brightness area's subsection map, and the color distortion problems caused by the traditional method of de-hazing are corrected. Besides, the orientation filter is adopted to optimize the atmospheric dissipation function and enhance the edge information of images so that the residual problems of de-hazing caused by large area of sky background can be overcome. Finally, an analysis of de-hazing is studied for the measured front image containing fog based on the actual agriculture intelligent navigation platform, and contrastive analyses of the method and traditional method are made by qualitative and quantitative de-hazing effect.

1 Traditional dark channel prior de-hazing

According to the research of literature [10], the atmospheric scattering model under the environment of fog can be expressed as:

$$I(x) = J(x)t(x) + A(1 - t(x)) \tag{1}$$

where I is haze image, A is the ambient light value of whole image as global constants, J is clarity image without haze, and t is media transmission image.

In the research, HE et al.[10] pointed out that, for any natural image J without haze, the dark channel should meet

$$J_{\text{dark}}(x) = \min_{y \in \Omega(x), c \in \{r,g,b\}} (\min J_c(y)) \to 0 \tag{2}$$

where $J_c(y)$ is one of R, G, B color channels, $\Omega(x)$ is the neighborhood of pixel center and the transmission value in its neighborhood is a constant, and $\Omega(x)$ is denoted as $\tilde{t}(x)$. Both ends of Eq. 1 are minimized simultaneously and the result can be shown as

$$\min_{y \in \Omega(x)} \left(\min_{c \in \{r,g,b\}} \frac{I_c(y)}{A_c} \right) = 1 + \tilde{t}(x) + \min_{y \in \Omega(x)} \left(\min_{c \in \{r,g,b\}} \frac{J_c(y)}{A_c} \right) \tilde{t}(x) \tag{3}$$

If A is the known constant, putting the Eq. 2 into Eq. 3, the transmission value can be roughly calculated as

$$\tilde{t}(x) = 1 - \min_{y \in \Omega(x)} \left(\min_{c \in \{r,g,b\}} \frac{I_c(y)}{A_c} \right) \tag{4}$$

Traditional method directly puts Eq. 4 into Eq. 1 to conduct the inversion de-hazing process, this method

leads to the obvious Halo effect and blocking effect. HE et al. [10] put forwards to use soft matting algorithm to optimize the effect of de-hazing well. Assuming that ambient light value of Eq. 4 has the equal values at each color channel, the mean value is $\overline{A}$, then the Eq. 4 can be further optimized as

$$\tilde{t}(x) = 1 - \frac{1}{\overline{A}} \min_{y \in \Omega(x)} \left(\min_{c \in \{r,g,b\}} \frac{I_c(y)}{A_c} \right) = 1 - \frac{I_{\text{dark}}(x)}{\overline{A}} \tag{5}$$

Eq. 5 is the widely adopted haze image dark channel at present, and the size of its values is proportional to the haze concentration. Through the definition of atmospheric dissipation function, the following formula can be obtained

$$V(x) = A(1 - t(x)) \tag{6}$$

$I_{\text{dark}}(x)$ can be express as preliminary estimation value of atmospheric dissipation function, therefore the optimization problem of transmission image and atmospheric dissipation function can be thought of as equivalent. Through transmission image $t(x)$ obtained by optimizing, the image obtained through de-hazing can be expressed as

$$J(x) = \frac{I(x) - \overline{A}}{\max(t(x), t')} + \overline{A} \tag{7}$$

where the setting of t' is mainly to overcome the possibility of that the denominator is zero, and t' is set equal to 0.05 in analysis of the paper.

2 Analysis for image segmentationmap method

When there is a large area of sky or white object, de-hazing effect of traditional dark channel prior method is not ideal. Although the application of orientation filter method can effectively improve this problem, it leads to the supersaturation and distortion of color. In order to solve this problem, first, the obtained image is segmented as areas of distant view and close shot to get the information of a minimum threshold value dark channel, and to conduct subsection map process based on the brightness information of image, then the preliminary prediction elimination value of atmospheric scattering function is given when the supersaturation and distortion of color are overcome. Second, the traditional orientation filter method is adopted to optimize the atmospheric scattering function, and the edge information of the image is further enhanced so that residual de-hazing problems caused by large area of sky background are improved.

2.1 Dark channel segmentation and subsection map of minimum threshold value

The key of dark channelde-hazing is to obtain the reasonable block neighborhood size, the size is greater, the edge information is poorer, and the Halo effect will be more serious. The smaller the neighborhood size is, the more accurate the edge information is, and the supersaturation and dark phenomenon of color after de-hazing is more serious. But through the minimum value operation of reasonable pixels R, G, B channel, the Halo effect can be effectively eliminated, and the supersaturationand dark problem is improved[14]. In order to optimize the dark channel, on the basis of the size of haze, the image is divided into two parts in this paper: close shot and distant view. Among them, the close shot image is less disturbed by big haze and the value of the dark channel will be smaller, and the distant view is more disturbed by haze and the value of dark channel will be bigger. Literature [13] points out that the close shot image can be approximated to image without haze and the value of the dark channel obtained though calculation is smaller, while the distant view image has bigger value of dark channel under the condition of haze. Therefore, the pixel level segmentation process of close shot and distant view for the original image with haze is conducted, the specific segmentation method can be shown as

$$I = \begin{cases} I_{\text{close}}(x) & (T < T_{\text{threshold}}) \\ I_{\text{distant}}(x) & (T \geqslant T_{\text{threshold}}) \end{cases} \tag{8}$$

where $T_{\text{threshold}}$ is the pixel threshold value of color channel R, G, B, $I_{\text{close}}(x)$ is close shot area, and $I_{\text{distant}}(x)$ is divided distant view area.

In order to further enhance the image segmentation accuracy of close shot and distant view, the information of channel R, G, B will be adopted to amend computational method of Eq. 5 before segmentation that the dark channel value is expressed as the form of the sum of minimum R, G, B color channel value and value of the dark channel of distant view, the calculation result is shown as

$$\begin{cases} \tilde{t}(x) = 1 - \dfrac{\tilde{I}_{\text{dark}}}{A} \\ \tilde{I}_{\text{dark}} = I_{\text{minc}} + I_{\text{dark}} \end{cases} \tag{9}$$

where I_{minc} is the R, G, B color minimum value channel information of $I_{\text{close}}(x)$, and I_{dark} is the dark channel information of $I_{\text{distance}}(x)$.

The effect comparison of segmentationde-hazing under different $T_{\text{threshold}}$ value is given in the Fig. 1.

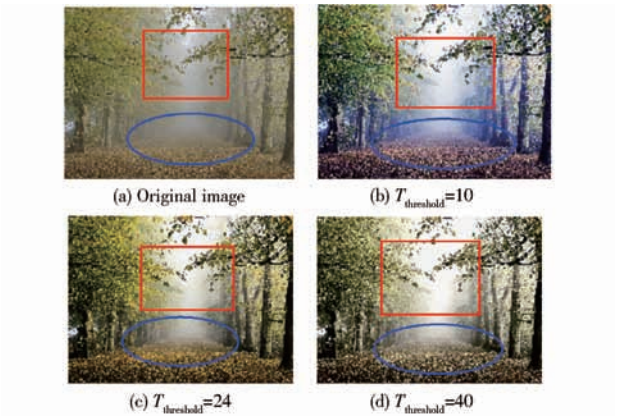

Fig. 1 De-hazing results with different threshold $T_{\text{threshold}}$

As shown in Fig. 1, when the appropriate threshold value $T_{\text{threshold}}$ is chosen, the expression of speed of view depth change can be well considered. The smaller threshold value is beneficial to deal with the image containing haze which the view depth change is gradual (ellipse section in Fig. 1), while larger threshold value is beneficial to deal with the image containing haze which has view depth mutation (the rectangular box in the Fig. 1). Processing results of Fig. 1b Fig. 1c and Fig. 1d show that the treatment effect at the joint of green plants and haze is poorer. The main reason is that large area of haze and white sky approximation region lead to the increase of dark channel of image so that color distortion is serious[15]. To solve this problem, on the basis of the early dark channel segmentation, subsection map processing is conducted based on the brightness information. Assuming that the least brightness value of image $\tilde{I}_{\text{dark}}$ is L, uniform subsection processing is conducted in the brightness range from L to 255 (the trisection is adopted in this paper, more subsection form can be divided in actual application based on accuracy and processing speed requirement). The subsection length is c, and the map in different range of $\tilde{I}_{\text{dark}}$ is compressed, the specific processing of map and compression can be shown as

$$\tilde{V}(x) = \begin{cases} \tilde{I}_{\text{dark}}(x)^{0.95} & (L+2c < \tilde{I}_{\text{dark}}(x) \leqslant 255) \\ \tilde{I}_{\text{dark}}(x)^{0.97} & (L+c < \tilde{I}_{\text{dark}}(x) \leqslant L+2c) \\ \tilde{I}_{\text{dark}}(x)^{0.98} & (L < \tilde{I}_{\text{dark}}(x) \leqslant L+c) \\ \tilde{I}_{\text{dark}}(x) & (0 \leqslant \tilde{I}_{\text{dark}}(x) \leqslant L) \end{cases} \tag{10}$$

where

$$c = \frac{255 - L}{3} \tag{11}$$

In the experimental analysis, the value of L is in the range from 150 to 215, the influence for the $\tilde{I}_{\text{dark}}$ is more gradual and the disturbance for image is minimum. In the subsequent analysis of this paper, L is set to 200 so that the error of sky or white object area corresponding mixed dark channel is decrease as far as possible.

By three period of uniform section map processing for original image of Fig. 1, the results are as shown in Fig. 2 (the results before the subsection map processing is called original results). The Fig. 2 shows the dark channel of image is well balanced and refined through map processing. From the overall results of the Fig. 2f, it can be seen that effect after processing can improve the color distortion well and further promote the clarity after de-hazing. Especially at the joint between haze and trees, the effect of de-hazing is obviously improved and enhanced, which promotes the differentiation of target in the image.

Fig. 2 De-hazing results of subsection mapping

2.2 Optimization analysis of orientation filter

From the analysis of Eq. 6 and Eq. 7, it can be seen that the optimization problems of transmitted image and atmospheric dissipation function can be summed as optimization processing of a same function in the process of actual image de-hazing. Due to the orientation filter has the characteristic of quick computing speed, can smooth image detailed information well and highlight the edge, which has got a faster development in the field of image de-hazing in recent years[16]. Therefore, in this paper, orientation filter is adopted to estimate the atmospheric dissipation function value V expressed by Eq. 6, the minimum channel value of image segmentation is adopted to calculate guide figure information (the information is as D). According to the traditional orientation filter linear model analysis, the output image can be expressed as

$$V_i = a_k D_i + b_k \quad (\forall i \in \omega_k) \tag{12}$$

where ω_k is the operation neighborhood produced by guide figure D, its center is pixel k, and the radius of calculation window is r. According to the researches of literature [17], the maximum similarity of detailed information between capture output figure and the guide image can be optimized when r is equal to 25. (a_k, b_k) is the constant value on ω_k, which is obtained by calculation though ensuring the largest connection between minimum output image V and the input image $\widetilde{V}$. Its cost function can be represented as

$$E(a_k, b_k) = \sum_{i \in \omega_k} [(a_k D_i + b_k - \widetilde{V}_i)^2 + \varepsilon a_k^2] \tag{13}$$

where ε is the optimal regular coefficient, literature [18] proves that the value of ε is not sensitive to the optimization result, ε is set as 10^{-3} in the subsequent calculation of this paper, the similarity measurement of V and $\widetilde{V}$ can be obtained by minimizing Eq. 13. Combining with the minimum dark channel information obtained from Eq. 9, the ambient light value A of image can be estimated. Combining with the optimal atmospheric scattering function V obtained from Eq. 2, the inverse calculation of de-hazing image can be achieved on the basis of Eq. 6.

3 Analyses of experimental results

3.1 Analyses of de-hazing effect of close shot and distant view image segmentation

In order to verify the effectiveness of this method, these gmentation de-hazing effect of public images for the literature [10] is analyzed by contrasting close shot and distant view. Depending on laboratory empirical analysis in the research, $T_{\text{threshold}}$ is 24 and the subsection map value is 3, and the specific experimental results are as shown in Fig. 3.

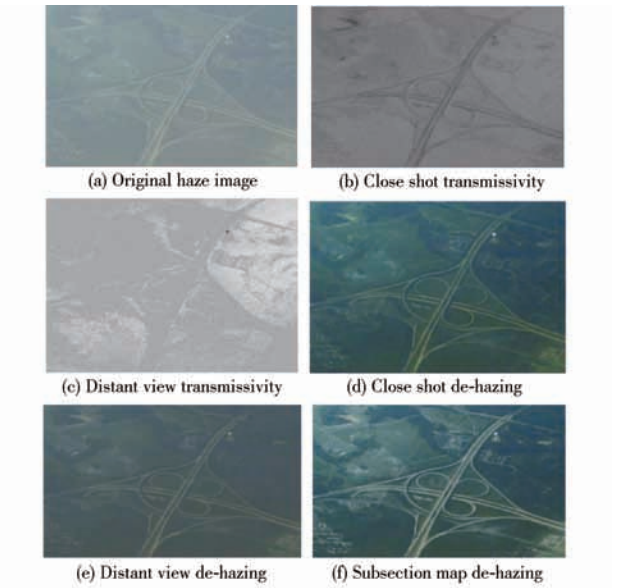

Fig. 3 De-hazing comparative analysis of segmentation

As shown in Fig. 3b and Fig. 3c, in the segmentation of close shot, its transmittance value at the details of dark channel is enhanced because of adopting the R, G, B channel minimum, and the extraction effect of transmissivity for large area analogous color information is enhanced in the segmentation of distant view. From Fig. 3d and Fig. 3e, it can be seen that the segmentation of close shot pixel level significantly enhances the clarity of image after de-hazing, compared with Fig. 3d, the subsection map effect in Fig. 3f further enhances the clarity of image de-hazing, which illustrate that the method of this paper has better de-hazing effect.

3.2 Actual experimental analysis of de-hazing effect for video navigation

In order to verify thede-hazing effect of visual navigation for this method in haze weather, for the images containing haze actually collected, two groups of experimental analysis are conducted.

Firstly, the de-hazing effect of image is qualitatively analyzed, and the de-hazing effect and the histogram distribution characteristics of corresponding R, G, B channel are given respectively.

Subsequently, the continuous images containing haze with 138 frames are carried out quantitative contrastive

analyses. These include contrast ratio improvement quantity e, color naturalness index (CNI), color colorfulness index (CCI) of images before and after processing, and the comprehensive indexes of image de-hazing proposed by literature [7] and computing time.

Finally, in order to ensure the effectiveness and fairness of the analysis, the unified pixels normalized processing of the tested images is conducted before de-hazing processing of the front images. The size of all processing images is set as multiplying 250 pixels and 340 pixels. For comparing the effectiveness of the method for this paper, the traditional orientation filter method, DCPR method and the method of this paper are respectively adopted to carry out the comparative analysis of them in the experiment, and the qualitative description of R, G, B frequency distribution before and after de-hazing is analyzed.

The test effect of de-hazing in the first group of images is shown as Fig. 4. As can be seen from the Fig. 4, the video images of this group has the characteristics of a deeper view depth, brightness, and low contrast ratio, the distribution range of pixel values is narrow and the number of pixels points for high pixel values is less, which is reflected in the histogram.

When tractor is driving on the field or road, the road commonly has a long extensibility, which is reflected in the image is that the view depth of image is deeper generally, so the image is selected to reflect the situation very well as shown in Fig. 4a. At the same time, the haze concentration of image before de-hazing in the figure is not entirely uniform, the haze concentration of closes hot and area with deeper view depth has significant differences, which conforms to the actual situation of distribution of haze on roads. So using this image to conduct algorithm test will help compare the effectiveness of each algorithm.

As shown in Fig. 4b, the orientation image filtering method has good smoothness for the image de-hazing, but it doesn't significantly improve contrast ration of image.

DCPR fails to significantly improve contrast ration of image. From Fig. 4c, it can be seen that obvious color distortion and the phenomenon of white edge appear, and artifacts phenomenon produce.

According to Fig. 4d, it is clear that the color distortion and the phenomenon of white edge do not occur while contrast and clarity of images are improved for the method of this paper.

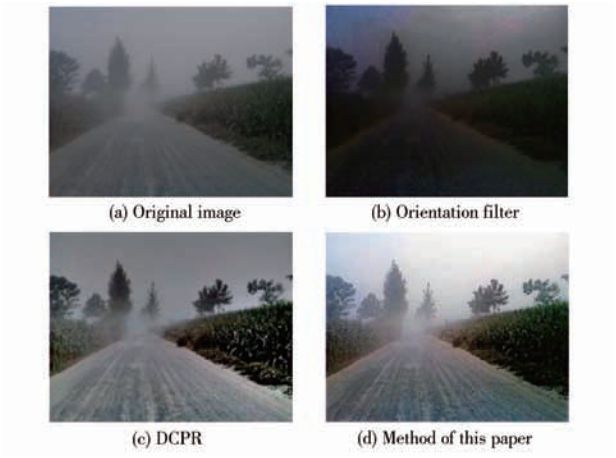

Fig. 4 De-hazing results of different methods

Fig. 5 shows the frequency distribution curve of R, G, B channel color histogram for each method after de-hazing. The frequency histogram distribution of image without de-hazing is narrow and the differences of R, G, B channel histogram are bigger, which is beneficial to conduct segmentation and calculate Eq. 9. After de-hazing processing, the area of R, G, B channel is uniform and de-hazing effect is better, then the color distribution of the three channels is more homogeneous and color frequency distribution of channel is wider. As shown in Fig. 5d, the color distribution of R, G, B channel after being processed by the method of this paper gets more uniform and mitigatory.

The tested video sequence in the second group is shown in Fig. 6. Compared with the first group, the tested sequence in this group has high brightness information, but the concentration of close shot is lower and the concentration of distant view is bigger.

From Fig. 7a, it can be seen that the R, G, B histogram is wider, but the difference among three colors channel frequency are bigger and the distinguish ability of background is worse. From the test results of Fig. 6, we can see that the oriented filtering and DCPR method eliminate the influence of haze to a certain extent and the latter have relatively better de-hazing effect.

As shown in Fig. 7b and Fig. 7c, the relative difference value of latter curve reduces. Neither the two methods enhance the performance of highlight for roads, so they cannot satisfy the needs from automatic navigation.

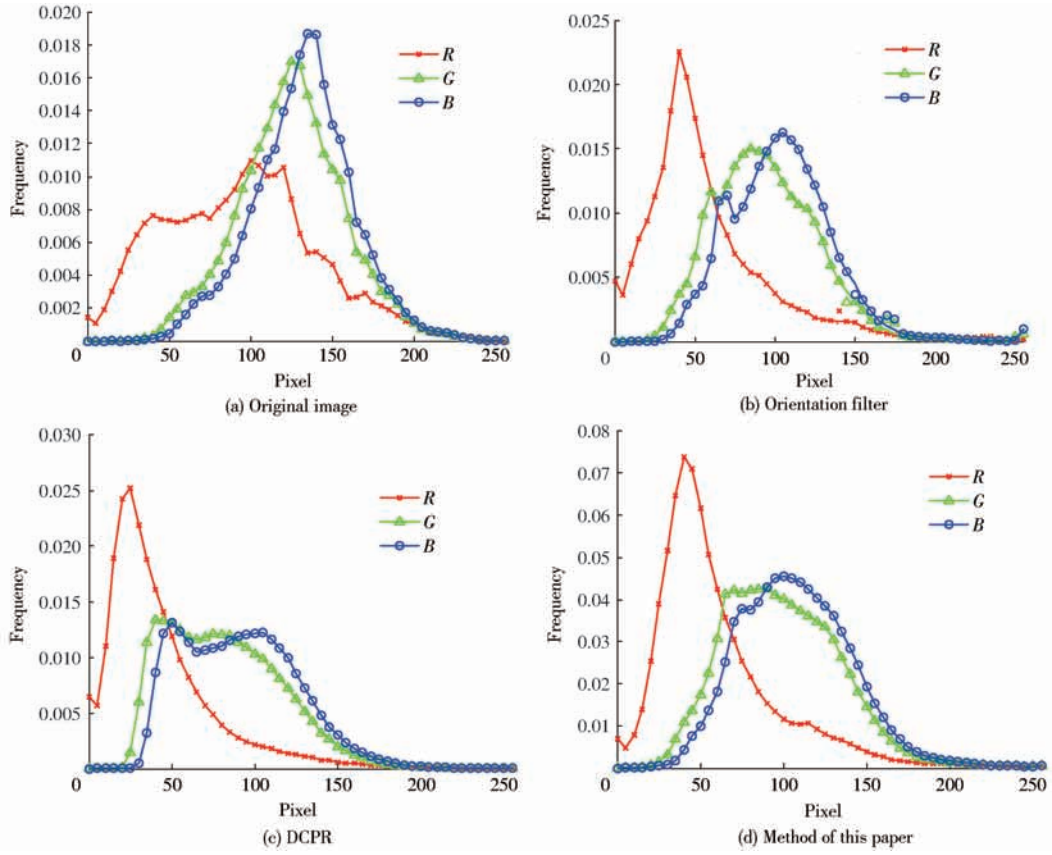

Fig. 5 R, G and B histograms

Fig. 6 De-hazing results of different methods

Due to the method of this paper adopts distant view and close shot segmentation method, which enhances the processing de-hazing ability for image details. At the same time, the subsection map methods highlights the contour information of road, so its processing effect is obviously superior to other methods as shown in Fig. 6d. From Fig. 7d, we can also see that R, G, B curve after being processed by this method is further broadened so that color curves occupy more pixel range, and the discrim ability of details are enhanced.

3.3 Quantitative comparative analysis for de-hazing effect

The analyses in section 3.1 and section 3.2 are mainly based on the external pattern of manifestation for images to conduct subjective qualitative analysis, this kind of evaluating effect doesn't have the universal evaluation effect because it is vulnerable to the individual subjective conditions. For this part, mainly aiming at the two sets of video image collected, under the same standard, the quantitative analysis of the image index to the actual de-hazing effect is conducted. For the comparative analysis for the CNI, CCI, CNC index and the time-consuming respectively, the specific effects of comparison are shown as Tab. 1 and Tab. 2.

From Tab. 1 and Tab. 2, it can be seen that the CNC index of the method in this paper has a maximum value, the effect after de-hazing reach the best, meanwhile the method in this paper and traditional orientation filter method keep the lower time-consuming. The main reason is that orientation filter method can limit the effective calculation scope and features space so that the instantaneity of calculation is guaranteed. At the same time, the instantaneity of algorithm is further improved because the method in this paper adopts the segmented uniform processing

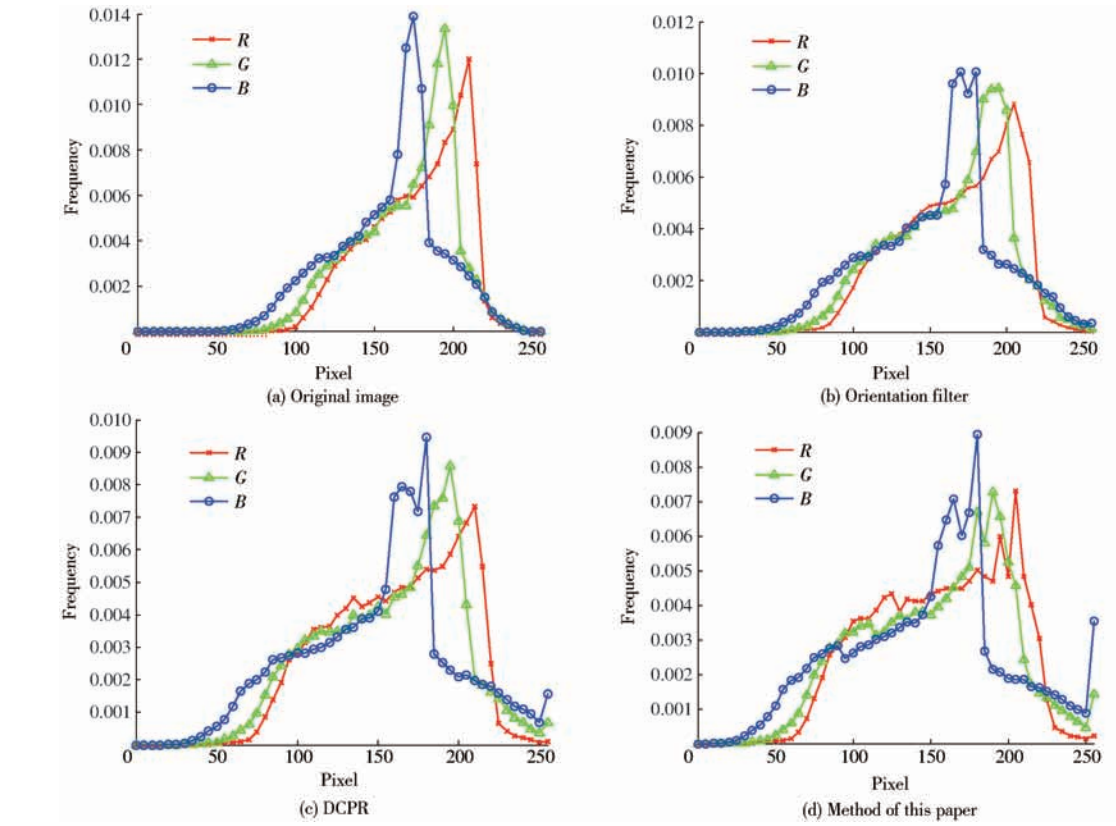

Fig. 7 R, G and B histograms

method. The time-consuming of this method is 0.209 s and 0.535 s that is less than traditional orientation filter method. Synthesizing the overall performance index, we can see that the method of this paper has better instantaneity and de-hazing effect.

Tab. 1 De-hazing performance analysis of the first set image sequence

De-hazing method	Index of quantitative performance				
	e	CNI	CCI	CNC	time-consuming/s
Orientation filter	1.594	0.564	0.018	0.864	0.629
DCPR	1.545	0.701	0.014	1.086	0.553
Method of this paper	1.786	0.803	0.058	1.375	0.209

Tab. 2 De-hazing performance analysis of the second set image sequence

De-hazing method	Index of quantitative performance				
	e	CNI	CCI	CNC	time-consuming/s
Orientation filter	2.007	0.501	0.019	0.745	1.508
DCPR	1.996	0.623	0.023	1.002	1.074
Method of this paper	2.134	0.685	0.049	1.293	0.535

4 Conclusions

(1) Asegmentation method of close shot and distant view area based on the size of haze is presented, and the method of pixel dark channel threshold value is adopted to segment close shot and distant view area.

(2) Asubsection map de-hazing method based on brightness information is proposed, which effectively improve the color distortion problem caused by traditional de-hazing method.

(3) The orientation filter is adopted topredict atmospheric dissipation function, which effectively enhance the edge information of image, so the residual problem caused by a large area of sky background is overcome to a certain extent.

(4) The experiments show that the method of this paper has higher precision and instantaneity for de-hazing. Under the actual tested complex farming environment, for two set of video images, the aggregative index of de-hazing was improve by 28.9% and 28.9% respectively and time-consuming was reduce by 34.4% and 53.9% respectively. However, it is still some insufficient places for the method in this paper, such as the determination of segmentation threshold value of close shot and distant view area is on the basis of experienced analysis of images obtained. In the following study, a closed-loop control relationship between quantitative analysis standards and threshold value segmentation will try to be established,

which will provide a real-time and effective adaptive threshold value segmentation method for the actual adaptive navigation application.

References

[1] LI B, WANG M H. In-field recognition and navigation path extraction for pineapple harvesting robots [J]. Intelligent Automation & Soft Computing, 2013, 19(1): 9 – 20.

[2] JI W, ZHAO D A, CHENG F Y, et al. Automatic recognition vision system guided for apple harvesting robot [J]. Computers and Electrical Engineering, 2012, 38(5): 1186 – 1195.

[3] WEI X Q, JIA K, LAN J H, et al. Automatic method of fruit object extraction under complex agricultural background for vision system of fruit picking robot [J]. Optik, 2014, 125(19): 5684 – 5689.

[4] TANG J L, JING X, HE D J, et al. Visual navigation control for agricultural robot using serial BP neural network[J]. Transactions of the CSAE, 2011, 27(2): 194 – 198.

[5] LI J B, ChEN B Q, LIU Y. Image detection method of navigation route of cotton plastic film mulch planter[J]. Transactions of the Chinese Society for Agricultural Machinery, 2014, 45(1):40 – 45. (in Chinese)

[6] ZHANG Zhengming, LU Wei, LU Jingxia. Dehazing method based on fast pseudosphere filtering for visual navigation of intelligent tractor in haze weather scene[J]. Robot, 2015,37(5):603 – 613. (in Chinese)

[7] WU Di, ZHU Qingsong. The latest research progress of image dehazing [J]. Acta Automatica Sinica, 2015, 41(2): 221 – 239.

[8] SHI Z W, LONG J, TANG W, et al. Single image dehazing in inhomogeneous atmosphere [J]. Optik International Journal for Light and Electron Optics, 2014, 125(15): 3868 – 3875.

[9] YU Jing, LI Dapeng, LIAO Qingmin. Physics-based fast single image fog removal [J]. Acta Automatica Sinica, 2011, 37(2):143 – 149. (in Chinese)

[10] HE K M, SUN J, TANG X O. Single image haze removal using dark channel prior[C] // Proceedings of the 2009 IEEE Conference on Computer Vision and Pattern Recognition, 2009: 1956 – 1963.

[11] HE K M, SUN J, TANG X O. Guided image filtering [J]. IEEE Transactions on Pattern Analysis and Machine Intelligence,2013, 35(6): 1397 – 1409.

[12] ZHANG Xiaogang, TANG Meiling, CHEN Hua, et al. A de-hazing method in single image based on double area filter and image fusion [J]. Acta Automatica Sinica, 2014,40(8): 1733 – 1739. (in Chinese)

[13] LIU Haibo, YANG Jie, WU Zhengping, et al. A fast single image dehazing method based on dark channel prior and Retinex theory[J]. Acta Automatica Sinica, 2015, 41(7): 1264 – 1273. (in Chinese)

[14] ZHOU Z Y, ZHANG Z G, LUO X W. A fuzzy path preview algorithm for the rice transplanting robot navigation system [J]. Journal of Software, 2014, 9(4): 881 – 888.

[15] WANG Y K, FAN C T. Single image defogging by multiscale depth fusion [J]. IEEE Transactions on Image Processing, 2014,23(11): 4826 – 4837.

[16] RUI Yibin, LI Peng, SUN Jintao. Method of removing fog effect from images [J]. Computer Applications, 2006, 26(1):154 – 156. (in Chinese)

[17] HE K, SUN J, TANG X. Single image haze removal using dark channel prior [J]. IEEE Transactions on Pattern Analysis and Machine Intelligence, 2011, 33(12): 2341 – 2353.

doi:10.6041/j.issn.1000-1298.2016.11.004

基于图像分割映射的农业机器人视觉去雾方法

姜德晶[1]　王树臣[1]　曾　勇[1,2]　孙　涛[1,3]　秦录芳[1]

(1.徐州工程学院机电工程学院,徐州 221111;2.盐城工学院机电学院,盐城 224003;
3.南京航空航天大学机电学院,南京 210016)

摘要:视觉导航农业机器人在雾天作业容易受前端含雾图像的影响,严重时无法有效工作。提出了一种基于图像分割映射的农业机器人视觉去雾方法。对前端采集图像进行近景与远景区域分割,并通过亮度信息的分段映射获取大气散射函数的预测估计值;采用导向滤波对大气散射函数的估计值进行优化,进一步增强图像的边缘信息,改善大面积天空背景引起的去雾残留问题。基于实际的农业智能导航平台对实测的含雾前端图像进行了去雾分析,并同传统的去雾方法进行了综合比较,显示所提方法具有较高的去雾精度和实时性。两段视频的图像去雾综合指标分别改善了 28.9% 和 29.1%,时间消耗分别减少了 34.4% 和 53.9%。

关键词:农业机器人;视觉导航;图像去雾;分割映射;导向滤波

中图分类号:TP391　　**文献标识码**:A　　**文章编号**:1000-1298(2016)11-0025-07

Agricultural Robot Visual De-hazing Method Based on Image Segmentation Map

Jiang Dejing[1]　Wang Shuchen[1]　Zeng Yong[1,2]　Sun Tao[1,3]　Qing Lufang[1]

(1. *School of Mechanical and Electrical Engineering*, *Xuzhou Institute of Technology*, *Xuzhou* 221111, *China*
2. *School of Mechanical and Electrical Engineering*, *Yancheng Institute of Technology*, *Yancheng* 224003, *China*
3. *College of Mechanical and Electrical Engineering*, *Nanjing University of Aeronautics & Astronautics*, *Nanjing* 210016, *China*)

Abstract: Because of the extensive flexibility and accuracy, visual navigation technology has been widely used in the field of agriculture intelligent navigation, and many effective machine vision navigation application cases were developed. But under the condition of heavy fog, visual navigation precision is greatly decreased and the processing time in the front image is largely increased, which due to unable to obtain clear front image recently. If the front image interference by the fog is bigger, and image enhancement and recovery effect is not obvious, then it will cause navigation function failure, which results in unable to effectively positioning and navigation. And even it cannot work in serious. In order to solve this problem, this paper proposed an agricultural robot visual de-hazing method based on image segmentation map. First of all, this paper adopted the front end image blurring vision and regional segmentation, and got the atmospheric scattering function prediction value based on the segmentation map through the image brightness information. Second, the method optimized the atmospheric scattering function estimation value based on the orientation filter, which enhanced the image edge information, and further improved the fog residual problem caused by the large sky background. Finally, the front-end image de-hazing experiment was conducted based on the actual agriculture intelligent navigation platform, and the results were compared with traditional de-hazing method. The results showed that the method had high precision and real-time performance. The image de-hazing integrated indicators were improved by 28.9% and 29.1% respectively of two part of the video, and the time consumption was improved by 34.4% and 53.9% respectively.

Key words: agricultural robot; visual navigation; image de-hazing; segmentation map; orientation filter

收稿日期:2016-06-02　修回日期:2016-09-05

基金项目:国家自然科学基金项目(51405418)、江苏省科技计划项目(BC20140071)和徐州市科技计划项目(KC14GM047)

作者简介:姜德晶(1967—),女,实验师,主要从事控制工程、农业机械视觉导航技术研究,E-mail:j_dejing@163.com

引言

随着现代农业机械智能化的快速发展,农业机器人广泛应用在农作物收获[1]、耕作施肥[2]以及水果采摘[3]等场合,大幅提升了现代农业的安全性和效率[4]。其中,基于机器视觉导航技术的智能农业机器人因操作方便、使用灵活,近年来得到了快速发展和应用[5],但是在雨、雪、雾等复杂天气条件下作业时,由于采集图像的退化、内容模糊、对比度降低等原因,导致路径识别精度降低,严重情况下还会引起控制系统紊乱,无法进行有效作业。因此,如何改善和提高雨、雪、雾天气条件下视觉图像的有效性,是目前视觉导航机器人面临的挑战和发展瓶颈。

近年来,研究人员将图像去雾技术引入到视觉导航系统[6],有效改善了雨、雪、雾天气下的机器人作业精度。根据图像去雾的实现手段,可以将当前的研究方法大致分为 2 类[7]:一类是基于传统图像增强的方法,如 Retinex 算法[8]。该类方法的优点是可以利用现有的图像增强处理方法,凸显图像中的目标特征和信息,但是忽略了图像退化的原因,在增强的过程中丢失了部分有用信息,使图像失真;另一类是基于物理模型的方法,该类方法深入分析退化机理,构建大气散射函数模型,通过函数反演恢复降质前的图像。由于该类方法考虑了大雾引起图像降质的机理,去雾效果较好,图像信息保存完整[9]。如 HE 等[10]提出的暗通道先验方法,由于该方法利用了图像的统计信息,实现手段简单、去雾效果好,目前成为图像去雾方法的研究热点,但是该方法的软抠图处理增加了算法的运算损耗,无法适应视觉导航系统对实时性的需求。在此基础上,文献[11]提出采用导向滤波取代软抠图方法,但是在大面积天空背景条件下,去雾效果较差;文献[12]通过利用中值滤波对大气耗散函数进行预估计,有效改善了软抠图的缺陷,但是滤波导向的模糊问题限制了改善效果;文献[13]将两类方法进行了融合,实现了暗通道先验和 Retinex 联合去雾,进一步提升了去雾效果。虽然目前的研究方法一定程度上改善了图像的去雾效果,为图像去雾提供了有效的思路,但是去雾后丢失了图像的部分细节信息,特别是在大面积天空背景以及大雾与目标图像的结合部分,容易引起较大的噪声干扰,降低图像的信噪比。这对于在复杂环境下作业的农业机器人导航系统而言,是十分不利的。针对这一问题,本文提出一种基于图像分割映射的农业机器人视觉去雾方法。基于图像含雾大小进行近景与远景分割,并通过亮度区域的分段映射对大气耗散函数进行初步的预测估计,修正传统方法去雾引起的颜色畸变问题;采用导向滤波对大气耗散函数进行优化处理,增强图像边缘信息,克服大面积天空背景引起的去雾残留问题。基于实际的农业智能导航平台对实测的含雾前端图像进行去雾分析,并将去雾效果同传统的去雾方法进行定性和定量的对比分析。

1 传统暗通道先验去雾

根据文献[10]的研究,可将大雾环境下的大气散射模型表示为

$$I(x)=J(x)t(x)+A(1-t(x)) \tag{1}$$

式中 I——雾霾图像

A——全幅图像的环境光值,为全局常量

J——清晰无雾图像

t——媒介传输图像

HE 等[10]在研究中指出,对于任意一幅自然无雾图像 J,其暗通道应该满足

$$J_{\text{dark}}(x)=\min_{y\in\Omega(x),c\in\{r,g,b\}}(\min J_c(y))\to 0 \tag{2}$$

式中 $J_c(y)$——$J(y)$的某一个 R、G、B 颜色通道

$\Omega(x)$——像素点中心的邻域

且在其邻域内的传输值为常数,记为 $\tilde{t}(x)$,对式(1)两端同时进行最小化处理可以得到

$$\min_{y\in\Omega(x)}\left(\min_{c\in\{r,g,b\}}\frac{I_c(y)}{A_c}\right)=1+\tilde{t}(x)+\min_{y\in\Omega(x)}\left(\min_{c\in\{r,g,b\}}\frac{J_c(y)}{A_c}\right)\tilde{t}(x) \tag{3}$$

如果 A 为已知常量,将式(2)代入式(3)可粗略计算出传输值为

$$\tilde{t}(x)=1-\min_{y\in\Omega(x)}\left(\min_{c\in\{r,g,b\}}\frac{I_c(y)}{A_c}\right) \tag{4}$$

传统方法直接采用式(4)代入式(1)进行反演去雾处理,这种方法导致了明显的 Halo 效应和块效应。HE 等[10]提出采用软抠图算法很好地优化了去雾效果。假设式(4)中的环境光值在每个颜色通道的值相等,均值为 $\overline{A}$,则式(4)可以进一步优化为

$$\tilde{t}(x)=1-\frac{1}{\overline{A}}\min_{y\in\Omega(x)}\left(\min_{c\in\{r,g,b\}}\frac{I_c(y)}{A_c}\right)=1-\frac{I_{\text{dark}}(x)}{\overline{A}} \tag{5}$$

式(5)即为目前广泛采用的雾霾图像暗通道,取值大小与雾霾浓度成正比。通过大气耗散函数的定义

$$V(x)=A(1-t(x)) \tag{6}$$

可知,$I_{\text{dark}}(x)$可表示大气耗散函数的初步估计值,因此,传输图像的优化问题和大气耗散函数的优化问题可以视为等价。通过优化获取的传输图像 $t(x)$可以将去雾获取的图像表示为

$$J(x)=\frac{I(x)-\overline{A}}{\max(t(x),t')}+\overline{A} \tag{7}$$

式中，t'的设置主要是克服分母为零的可能，在分析中本文设置 $t'=0.05$。

2　图像分割映射方法分析

传统暗通道先验方法对于存在大面积天空或白色物体情况下的去雾效果不理想，虽然导向滤波方法的应用有效地改善了这一问题，但却引入了颜色过饱和畸变。针对这一问题，本文首先对获取的图像进行远景和近景区域分割，获取最小阈值暗通道信息，并基于图像亮度信息进行分段映射处理，在克服颜色过饱和畸变的同时，给出了大气散射函数的初步预测估计值；然后采用传统的导向滤波方法对大气散射函数进行优化，进一步增强图像的边缘信息，改善了大面积天空背景引起的去雾残留问题。

2.1　最小值阈值暗通道分割及分段映射

暗通道去雾的关键是获取合理的块状邻域大小，邻域尺寸越大，边缘信息越差，Halo 效应越严重；邻域尺寸越小，边缘信息越精确，去雾后颜色过饱和与昏暗现象越严重。但通过合理的像素点 R、G、B 通道极小值运算，可以有效消除 Halo 效应，改善过饱和和昏暗问题[14]。为了进行暗通道的优化，本文基于图像含雾大小，将图像分割为近景和远景部分，其中近景图像受大雾的干扰较小，暗通道值较小；而远景图像，雾气干扰较大，暗通道值较大。文献[13]指出，近景图像可以近似为无雾图像，计算获取的暗通道值较小；而远景图像在有雾霾的情况下具有较大的暗通道值。因此，本文基于对原始含雾图像进行像素级的远、近景分割处理，具体的分割方法为

$$I=\begin{cases}I_{\text{close}}(x) & (T<T_{\text{threshold}})\\ I_{\text{distant}}(x) & (T\geqslant T_{\text{threshold}})\end{cases} \tag{8}$$

式中　$T_{\text{threshold}}$——颜色通道 R、G、B 的像素集合初始阈值

$I_{\text{close}}(x)$——近景区域

$I_{\text{distant}}(x)$——划分的远景区域

为进一步增强图像远近分割的精确性，分割之前采用 R、G、B 通道信息对式(5)的计算方法进行修正，将暗通道值表示为最小 R、G、B 颜色通道值与远景暗通道值之和的形式，计算结果为

$$\begin{cases}\check{t}(x)=1-\dfrac{\check{I}_{\text{dark}}}{\overline{A}}\\ \check{I}_{\text{dark}}=I_{\text{minc}}+I_{\text{dark}}\end{cases} \tag{9}$$

式中　I_{minc}——$I_{\text{close}}(x)$ 的 R、G、B 颜色最小值通道信息

I_{dark}——$I_{\text{distant}}(x)$ 的暗通道信息

图 1 中给出了在不同 $T_{\text{threshold}}$ 取值情况下分割去雾效果对比。

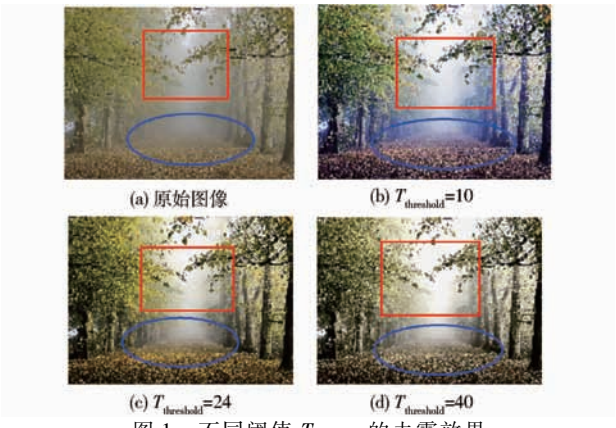

图 1　不同阈值 $T_{\text{threshold}}$ 的去雾效果

Fig. 1　De-hazing results with different threshold $T_{\text{threshold}}$

从图 1 可以看出，在选择合适的 $T_{\text{threshold}}$ 阈值情况下，能够很好地兼顾景深变化快慢的表达，较小的阈值有益于处理景深变化缓和含雾图像(图中椭圆标记部分)，而较大的阈值有利于处理景深突变的含雾图像(图中矩形方框标记部分)。图 1b、1c、1d 的处理结果可以看出在绿色植物和大雾连接处的处理效果较差。主要原因是大面积雾霾和天空白色近似区域导致图像暗通道增加，颜色失真严重[15]。针对这种情况，在前期暗通道分割的基础上，基于亮度信息进行分段映射处理。假设图像 $\check{I}_{\text{dark}}$ 的最小亮度为 L，在 L 到 255 的亮度区间内进行均匀分段处理(本文采用三等分，实际应用中可以在精度与处理速度需求中进行折中，划分更多的分段形式)，分段长度记为 c，并针对 $\check{I}_{\text{dark}}$ 不同区间的映射进行压缩处理，具体的映射和压缩过程为

$$\tilde{V}(x)=\begin{cases}\check{I}_{\text{dark}}(x)^{0.95} & (L+2c<\check{I}_{\text{dark}}(x)\leqslant 255)\\ \check{I}_{\text{dark}}(x)^{0.97} & (L+c<\check{I}_{\text{dark}}(x)\leqslant L+2c)\\ \check{I}_{\text{dark}}(x)^{0.98} & (L<\check{I}_{\text{dark}}(x)\leqslant L+c)\\ \check{I}_{\text{dark}}(x) & (0\leqslant\check{I}_{\text{dark}}(x)\leqslant L)\end{cases} \tag{10}$$

其中

$$c=\frac{255-L}{3} \tag{11}$$

实验分析中 L 取值在 150 ~ 215 范围内，对 $\check{I}_{\text{dark}}$ 的影响比较平缓，且对图像干扰最小，本文在后续分析中取 $L=200$，尽可能地减小天空或白色物体区域相应混合暗通道的误差。

图 2 给出了图 1 输入的原始图像进行 3 段均匀分段映射处理后的效果，分段映射处理前的为“原

始效果”,从图中可以看出,经过映射处理以后,图像的暗通道得到了很好均衡和细化,从图 2f 的整体效果可以看出,处理后的效果能够很好地改善颜色畸变效应,且进一步提升了去雾后的清晰度,尤其是雾霾与树木相结合的部位,去雾效果明显改善和增强,提升了图像中目标的区分度。

图 2 分段映射去雾效果

Fig. 2 De-hazing results of subsection mapping

2.2 导向滤波的优化分析

通过式(6)、(7)的分析可以看出,实际图像去雾过程中,传输图像的优化和大气耗散函数的优化问题可以归结为同一个函数的优化处理。由于导向滤波具有计算速度快,且能够很好地平滑图像细节信息,凸显边缘,近年来在图像去雾领域得到较快的发展[16]。因此,本文采用导向滤波估计式(6)所示的大气耗散函数值 V,其中的引导图信息利用图像分割的最小值通道,计算中采用 D 表示。根据传统的导向滤波线性模型分析,可将输出图像表示为

$$V_i = a_k D_i + b_k \quad (\forall i \in \omega_k) \tag{12}$$

式中,ω_k 为引导图 D 产生的操作邻域,其中心为像素 k,计算窗口的半径为 r,根据文献[17]的研究,在 $r=25$ 的时候能够最优化捕获输出图像与引导图像之间细节信息的最大相似度,(a_k, b_k) 为操作邻域 ω_k 上的常数值,该系数主要是通过保证最小化输出图像 V 同输入图像 $\widetilde{V}$ 之间的最大关联性来计算获取,其代价函数可表示为

$$E(a_k, b_k) = \sum_{i \in \omega_k} [(a_k D_i + b_k - \widetilde{V}_i)^2 + \varepsilon a_k^2] \tag{13}$$

式中,ε 为优化的正则系数,文献[18]证明该系数值对结果优化不敏感,本文在后续的计算中取值 $\varepsilon = 10^{-3}$,通过式(13)的最小化可以获取 V 和 $\widetilde{V}$ 的相似度量值。结合式(9)获取的最小阈值暗通道信息可以估计出图像的环境光值 A,结合式(13)获取的优化后的大气散射函数 V,可以在式(6)的基础上反演计算出去雾图像。

3 实验结果分析

3.1 远近景图像分割去雾效果分析

为验证本文方法的有效性,首先针对文献[10]给出的公共含雾图像进行了远景与近景分割去雾效果对比分析。实验中分割阈值取值主要依据实验室经验分析,取值为 $T_{\text{threshold}} = 24$,分段映射值为 3,具体的实验结果如图 3 所示。

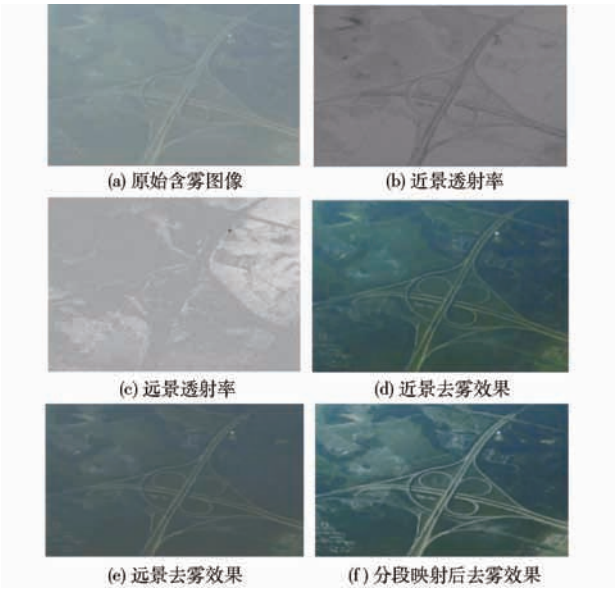

图 3 远近景分割去雾对比分析

Fig. 3 De-hazing comparative analysis of segmentation

从图 3b、3c 中可以看出,近景分割由于采用了 R、G、B 通道最小值,增强了暗通道细节处的透射率值,而远景分割增强了大面积类似颜色信息的透射率提取效果。从图 3d、3e 中可以看出,近景像素级的分割明显增强了图像去雾后的清晰度,同图 3d 相比较,图 3f 中的分段映射效果进一步增强了图像去雾的清晰度,说明本文方法具有较好的去雾效果。

3.2 视频导航去雾效果实验分析

为验证本文方法在雾霾天气下的视觉导航去雾效果,针对实际采集的含雾图像进行 2 组实验分析。首先,进行了图像去雾效果的定性分析,分别给出了去雾后的效果以及相应的 R、G、B 通道直方图分布特性;接着,针对采集的 138 帧连续含雾图像,进行了定量的对比分析,分别给予处理前后图像的对比度改善量 e、色彩自然度(color naturalness index, CNI)、颜色丰富程度(color colorfulness index, CCI)

以及文献[7]提出的图像去雾综合指标(CNC)和计算耗时 5 个方面进行了定量的对比分析。为了保证分析的有效性和公平性,在采集的前段图像进入去雾处理之前,对测试图像进行了统一的像素归一化处理,所有的处理图像大小设置为 250 像素 × 340 像素。为对比本文方法的有效性,实验中分别采用了传统导向滤波方法、DCPR 方法以及本文方法进行了对比分析,并对去雾前后的 RGB 频率分布进行定性描述分析。

第 1 组的去雾图像测试效果如图 4 所示。从图 4 中可以看出,该组视频图像具有较深景深、亮度、对比度低的特点,反映在直方图中为像素值的分布区间狭窄并且像素值高的像素点数量少。选取此图像作为测试图像的原因是拖拉机在田间及道路上行驶时,道路一般具有很长的延伸性,反映在图像中便是图像的景深一般较深,图 4a 很好地反映了这一情况。同时,图中的去雾前图像的雾气浓度并非完全均匀,近景处浓度与景深较深的区域雾气浓度有明显差异,这符合道路雾气分布的实际情况,使用此图像进行算法测试有助于对比各算法的有效性。测试结果表明,导向图滤波方法对图像去雾的平滑性好,但并未明显提高图像的对比度;DCPR 未能显著提高图像对比度,出现明显的色彩失真,而且出现了“白边”现象,产生了伪影现象;本文方法在提高图像对比度与清晰度的同时没有出现色彩失真及边缘白边现象,对暗原色去雾框架的算法有较大的改善。

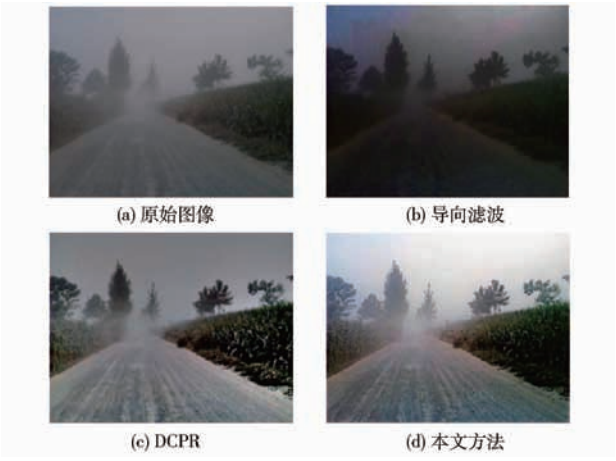

图 4　不同方法去雾效果

Fig. 4　De-hazing results of different methods

图 5 给出了每种方法去雾后的 R、G、B 通道颜色直方图的频率分布曲线。可以看出,含雾图像没有进行去雾处理之前频率直方图分布较窄,并且 R、G、B 通道的直方图差别较大,利于进行分割和式(9)的计算,进行去雾处理以后,R、G、B 通道区域均匀,且去雾效果越好,3 个通道的颜色分布越均衡,通道颜色的频率分布展宽,如图 5d 所示。经过本文方法处理以后的 R、G、B 通道的颜色分布更加均匀缓和。

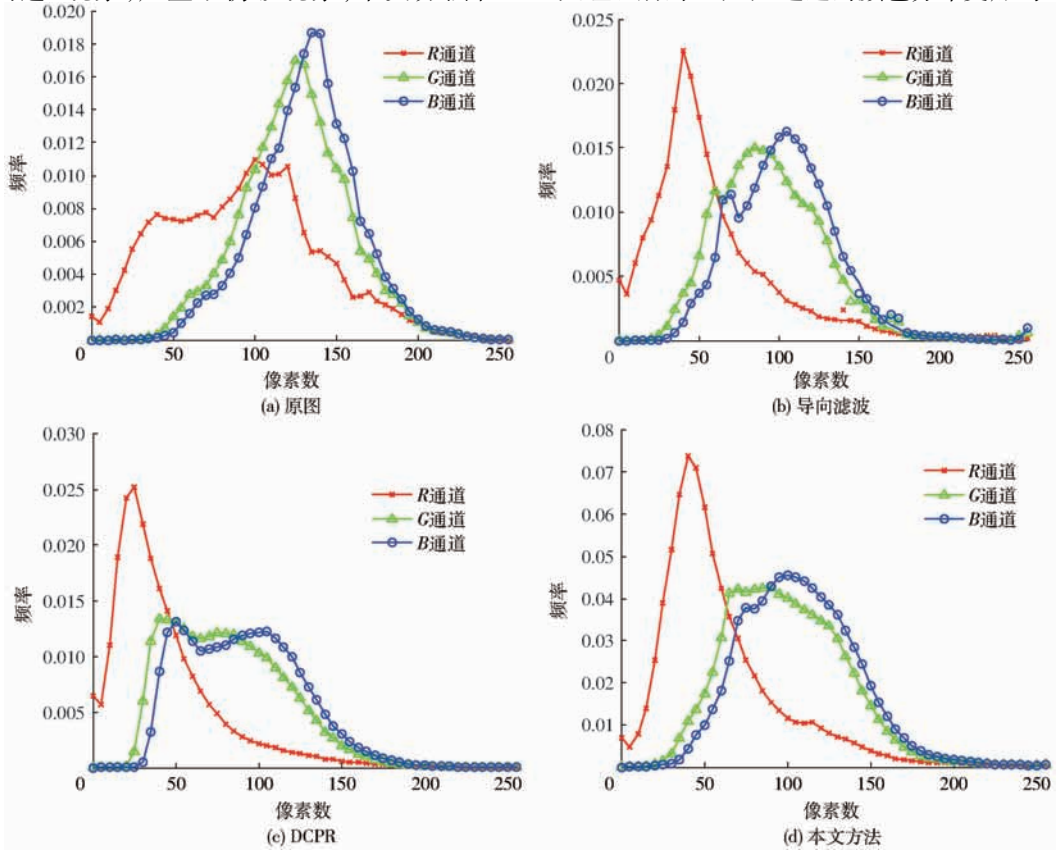

图 5　R、G、B 通道直方图

Fig. 5　R, G and B histograms

第 2 组测试视频序列如图 6 所示。该测试序列同第 1 组相比具有较高的亮度信息,但是近景浓度较低,远景浓度较大,从图 7a 中可以看出,该图像的 R、G、B 直方图较宽,但是 3 色通道频率差别较大,背景的可区分性较差。从图 6 中的测试结果可以看出,导向滤波与 DCPR 方法一定程度上去除了雾霾的影响,且后者具有相对较好的去雾效果,可以从图 7b、7c 的 R、G、B 通道曲线看出,后者曲线相对差值降低,但是 2 种方法都没有增强道路的凸显性能,因此无法满足自动导航的需求。但是本文方法由于采用了远近分割的方法增强了图像细节去雾的处理能力,同时,分段映射的方法凸显了道路轮廓信息,处理效果明显优于其他方法,具体如图 6d 所示,从图 7d 中也可以看出,本文方法处理后的 RGB 曲线进一步展宽,颜色曲线占据较多的像素范围,增强了细节区分度。

图 6 第 2 组测试视频不同方法去雾效果对比图

Fig. 6 De-hazing results of different methods

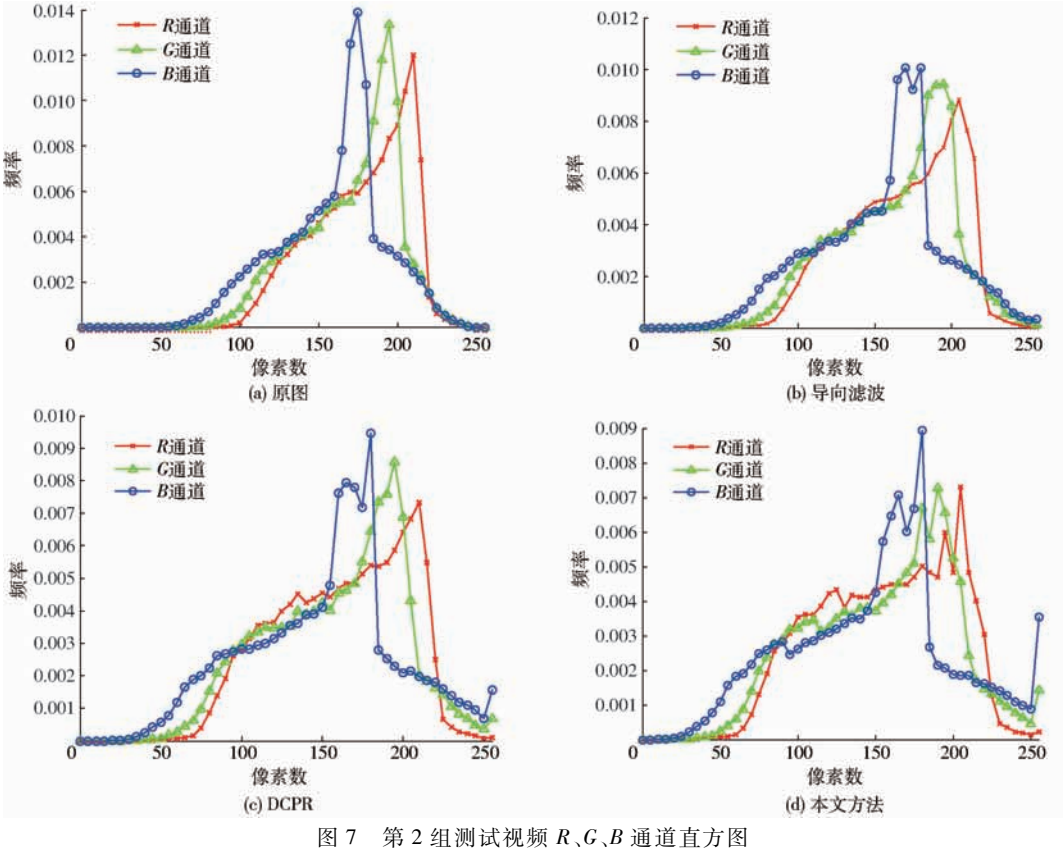

图 7 第 2 组测试视频 R、G、B 通道直方图

Fig. 7 R, G and B histograms

3.3 去雾效果定量比较分析

第 3.1 节与 3.2 节中的分析主要是基于图像的外在表现形式进行主观定性分析,由于这种评价效果容易受到个人主观条件的干扰、不具有普适的评价效果,该部分主要针对采集的 2 组视频图像,在相同的标准下,对实际的去雾效果进行了定量的图像指标分析。分别针对 e、CNI、CCI、CNC 指标以及计算的时间消耗进行了对比分析,具体的比较效果如表 1 和表 2 所示。

表 1 第 1 组图像序列去雾性能分析

Tab. 1 De-hazing performance analysis of the first set image sequence

去雾方法	定量性能指标				
	e	CNI	CCI	CNC	耗时/s
导向滤波	1.594	0.564	0.018	0.864	0.629
DCPR	1.545	0.701	0.014	1.086	0.553
本文方法	1.786	0.803	0.058	1.375	0.209

从表 1、表 2 中可以看出,本文方法的 CNC 指标具有最大值,去雾后的效果达到了最佳,同时本文算

表 2　第 2 组图像序列去雾性能分析

Tab. 2　De-hazing performance analysis of the second set image sequence

去雾方法	定量性能指标				
	e	CNI	CCI	CNC	耗时/s
导向滤波	2.007	0.501	0.019	0.745	1.508
DCPR	1.996	0.623	0.023	1.002	1.074
本文方法	2.134	0.685	0.049	1.293	0.535

法和传统导向滤波方法保持了较低的运算消耗，主要原因是导向滤波方法能够限制有效的运算范围和特征空间，保证运算的实时性，同时，因为本文方法采用了分段均匀处理的方法，进一步提升了算法的实时性，本文方法的时间消耗为 0.209 s 和 0.535 s，较传统的导向滤波去雾方法时间消耗有所降低。综合整体的性能指标可以看出，本文方法具有更好的实时性和去雾效果。

4　结论

（1）提出了一种基于含雾大小的远近景区域分割方法，采用像素暗通道阈值的方法进行远景与近景区域的分割处理。

（2）提出了基于亮度信息的分段映射暗通道去雾方法，有效改善了传统去雾方法引入的颜色畸变问题。

（3）采用导向滤波对大气耗散函数的预测估计，有效增强了图像的边缘信息，一定程度上克服了大面积天空背景引起的去雾残留问题。

（4）最后的实际测试实验表明，本文方法具有更高的去雾精度和实时性，在实际测试的复杂农业耕作环境下的两段视频图像去雾综合指标分别改善了 28.9% 和 29.1%，时间消耗分别减少了 34.4% 和 53.9%。但是，本文方法仍然有不足的地方，例如远近区域分割阈值的确定是基于获取图形的经验分析，在后续的研究中将试图建立定量分析标准与阈值分割的闭环控制关系，为实际的自适应导航应用提供实时有效的自适应阈值分割方法。

参　考　文　献

1　LI B, WANG M H. In-field recognition and navigation path extraction for pineapple harvesting robots[J]. Intelligent Automation & Soft Computing, 2013, 19(1): 9 – 20.

2　JI W, ZHAO D A, CHENG F Y, et al. Automatic recognition vision system guided for apple harvesting robot[J]. Computers and Electrical Engineering, 2012, 38(5): 1186 – 1195.

3　WEI X Q, JIA K, LAN J H, et al. Automatic method of fruit object extraction under complex agricultural background for vision system of fruit picking robot [J]. Optik, 2014, 125(19): 5684 – 5689.

4　TANG J L, JING X, HE D J, et al. Visual navigation control for agricultural robot using serial BP neural network [J]. Transactions of the CSAE, 2011, 27(2): 194 – 198.

5　李景彬，陈兵旗，刘阳. 棉花铺膜播种机导航路线图像检测方法[J]. 农业机械学报, 2014, 45(1): 40 – 45.
LI J B, ChEN B Q, LIU Y. Image detection method of navigation route of cotton plastic film mulch planter[J]. Transactions of the Chinese Society for Agricultural Machinery, 2014, 45(1):40 – 45. (in Chinese)

6　张征明，卢伟，陆静霞. 基于快速伪球滤波的智能拖拉机视觉导航中场景去雾方法[J]. 机器人，2015，37(5)：603 – 613.
ZHANG Zhengming, LU Wei, LU Jingxia. Dehazing method based on fast pseudosphere filtering for visual navigation of intelligent tractor in haze weather scene[J]. Robot, 2015, 37(5): 603 – 613. (in Chinese)

7　吴迪，朱青松. 图像去雾的最新研究进展[J]. 自动化学报，2015，41(2)：221 – 239.
WU Di, ZHU Qingsong. The latest research progress of image dehazing [J]. Acta Automatica Sinica, 2015, 41(2): 221 – 239.

8　SHI Z W, LONG J, TANG W, et al. Single image de-hazing in inhomogeneous atmosphere [J]. Optik International Journal for Light and Electron Optics, 2014, 125(15): 3868 – 3875.

9　禹晶，李大鹏，廖庆敏. 基于物理模型的快速单幅图像去雾方法[J]. 自动化学报，2011，37(2)：143 – 149.
YU Jing, LI Dapeng, LIAO Qingmin. Physics-based fast single image fog removal [J]. Acta Automatica Sinica, 2011, 37(2): 143 – 149. (in Chinese)

10　HE K M, SUN J, TANG X O. Single image haze removal using dark channel prior[C] // Proceedings of the 2009 IEEE Conference on Computer Vision and Pattern Recognition, 2009: 1956 – 1963.

11　HE K M, SUN J, TANG X O. Guided image filtering[J]. IEEE Transactions on Pattern Analysis and Machine Intelligence, 2013, 35(6): 1397 – 1409.

12　张小刚，唐美玲，陈华，等. 一种结合双区域滤波和图像融合的单幅图像去雾算法[J]. 自动化学报，2014，40(8)：1733 – 1739.
ZHANG Xiaogang, TANG Meiling, CHEN Hua, et al. A de-hazing method in single image based on double area filter and image fusion[J]. Acta Automatica Sinica, 2014, 40(8): 1733 – 1739. (in Chinese)

13　刘海波，杨杰，吴正平，等. 基于暗通道先验和 Retinex 理论的快速单幅图像去雾方法[J]. 自动化学报，2015，41(7)：1264 – 1273.
LIU Haibo, YANG Jie, WU Zhengping, et al. A fast single image dehazing method based on dark channel prior and Retinex theory[J]. Acta Automatica Sinica, 2015, 41(7): 1264 – 1273. (in Chinese)

14　ZHOU Z Y, ZHANG Z G, LUO X W. A fuzzy path preview algorithm for the rice transplanting robot navigation system[J]. Journal of Software, 2014, 9(4): 881 – 888.

15　WANG Y K, FAN C T. Single image defogging by multiscale depth fusion[J]. IEEE Transactions on Image Processing, 2014, 23(11): 4826 – 4837.

16　芮义斌，李鹏，孙锦涛. 一种图像去薄雾方法[J]. 计算机应用，2006，26(1)：154 – 156.
RUI Yibin, LI Peng, SUN Jintao. Method of removing fog effect from images [J]. Computer Applications, 2006, 26(1): 154 – 156. (in Chinese)

17　HE K, SUN J, TANG X. Single image haze removal using dark channel prior[J]. IEEE Transactions on Pattern Analysis and Machine Intelligence, 2011, 33(12): 2341 – 2353.